

# Energy-gap dynamics of superconducting NbN thin films studied by time-resolved terahertz spectroscopy

M. Beck,<sup>1</sup> M. Klammer,<sup>1</sup> S. Lang,<sup>1</sup> P. Leiderer,<sup>1</sup> V.V. Kabanov,<sup>2,3</sup> G. N. Gol'tsman,<sup>4</sup> and J. Demsar<sup>1,2,3</sup>

<sup>1</sup>*Dept. of Physics and Center for Applied Photonics, Univ. of Konstanz, D-78457, Germany*

<sup>2</sup>*Zukunftskolleg, Univ. of Konstanz, D-78457, Germany*

<sup>3</sup>*Complex Matter Dept., Jozef Stefan Institute, SI-1000, Slovenia and*

<sup>4</sup>*Moscow State Pedagogical University, Moscow, Russia*

Using time-domain Terahertz spectroscopy we performed direct studies of the photoinduced suppression and recovery of the superconducting gap in a conventional BCS superconductor NbN. Both processes are found to be strongly temperature and excitation density dependent. The analysis of the data with the established phenomenological Rothwarf-Taylor model enabled us to determine the bare quasiparticle recombination rate, the Cooper pair-breaking rate and the electron-phonon coupling constant,  $\lambda = 1.1 \pm 0.1$ , which is in excellent agreement with theoretical estimates.

PACS numbers: 78.47.J-, 74.40.Gh

Soon after the first tunneling experiments in superconductors (SCs) revealed that the quasiparticle (QP) tunneling can be qualitatively described in terms of the QP energy band picture, in which the SC can be treated similarly to a narrow gap semiconductor, it was realized that SCs can be used as detectors for far-infrared light [1]. Since real-world applications of SCs require an understanding of their properties under non-equilibrium conditions several attempts were made already in 1960's to determine the time scales and processes that govern the recovery of the SC state. It was soon realized [2] that the recombination process, where two QP recombine to form a Cooper pair, was dominated by the emission of phonons with  $\hbar\omega > 2\Delta$ ,  $\Delta$  being the SC gap. However, as pointed out by Rothwarf and Taylor [3], the re-absorption of  $\hbar\omega > 2\Delta$  phonons leads to the so called phonon bottleneck, where the recovery of the SC state is not governed by the bare recombination of two QPs into the condensate, but rather by the decay of  $\hbar\omega > 2\Delta$  phonons. The non-equilibrium state can be generated either by QP injection in tunnel junctions [2], or by excitation with photons of energy larger than  $2\Delta$ . In particular, due to the rapid development in the generation of ultrashort laser pulses and related femtosecond pump-probe techniques, the latter approach has enabled direct studies of carrier relaxation dynamics with femtosecond time resolution. Most of the work reported to date focussed on high- $T_c$  SCs; predominantly on cuprates [4–15] but more recently also on pnictides [16–19]. The main focus of the research was on the influence of the superconducting gap and the normal state pseudogap on the carrier relaxation dynamics [4–6, 8, 9, 20–22, 26]. One of the still controversial issues with cuprates is the effect of the d-wave gap on the relaxation phenomena, and the role of phonons, i.e. the existence [5, 15, 20] or absence [8, 9] of the phonon bottleneck in this class of SCs. Recently, systematic studies of the photoinduced melting of SC have been performed in cuprates [11–14]. Moreover, manipulation of the order parameter in  $\text{La}_{1.84}\text{Sr}_{0.16}\text{CuO}_4$  by applying intense Tera-

hertz (THz) electric fields along the c-axis has also been demonstrated [23]. Despite numerous studies in high- $T_c$  SCs, whose ground state properties are not well understood, only a few experiments on conventional BCS SCs exist [24–27], but no systematic study of dynamics as a function of temperature (T) and the absorbed energy density (A). Studies of non-equilibrium dynamics in conventional SCs are an important first step to understanding relaxation dynamics in more exotic SCs. Since for conventional BCS SC  $\Delta$  lies in the low-THz range, and can be resonantly probed by time domain THz spectroscopy (TDTS), the data interpretation should be less ambiguous.

In this Letter we report on the first detailed study of the SC state relaxation phenomena in a conventional SC NbN [28] over wide range of T and A. Utilizing the TDTS we have studied the T-dependence of its complex conductivity,  $\sigma(\omega)$ , as well as its T- and A-dependent dynamics following photoexcitation with a fs optical pulse. We show that  $\sigma(\omega)$  can be well fit to the prediction of the BCS theory [29], enabling direct studies of the temporal evolution of  $\Delta$ . Both, the Cooper pair breaking (CPB) and the SC state recovery were found to be T- and A-dependent, and could be well explained by the Rothwarf-Taylor (RT) phonon-bottleneck model [3, 20]. From the dependence of the CPB on A we were able to determine the microscopic QP recombination rate,  $R$ , as well as the value of the electron-phonon (e-ph) coupling constant,  $\lambda$ .

NbN thin films were deposited by dc magnetron sputtering on MgO substrates [31]. Films with thicknesses between 10-15 nm and  $T_c$  between 14.3-15.4 K ( $\Delta T_c = 0.19 - 0.17$  K) were investigated. The TDTS set-up was built around a 250 kHz amplified Ti:sapphire laser system, utilizing large area interdigitated photoconductive emitter for the generation of THz pulses [32], while the THz electric fields transmitted through the sample,  $E_{tr}(t')$ , and reference,  $E_{re}(t')$ , were detected using the Pockels effect in GaP. The real,  $\sigma_1(\omega)$ , and the imaginary,  $\sigma_2(\omega)$ , parts of the optical conductivity were deter-

mined using the appropriate Fresnel equations. In non-equilibrium experiments, the films were excited by 50 fs pulses at the carrier wavelength of 800 nm. The time evolution of the SC state as a function of  $t_d$ , the time delay of the THz pulse with respect to the optical excitation, was studied by either directly measuring  $\sigma(\omega, t_d)$  or by measuring the induced changes in the transmitted electric field,  $\Delta E_{tr}(t', t_d)$ , at a fixed  $t'$ . The latter, spectrally integrated traces, are particularly useful for studying dynamics at low excitations [7, 9, 26]. The THz beam diameter on the sample was  $\approx 1.5$  mm [30], while that of the photoexcitation beam was 4 mm, ensuring the homogeneous lateral excitation profile. From reflectivity and transmission of the films at 800 nm we determined the optical penetration depth  $l_{opt} \approx 12$  nm. The absorbed energy densities at the film surface,  $A$ , were calculated from the reflectivity and  $l_{opt}$  and are given in  $\text{mJ}/\text{cm}^3$ .

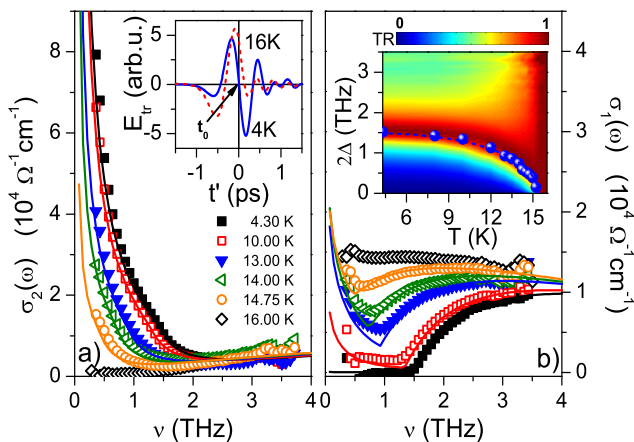


FIG. 1: (color online) The T-dependence of the a) imaginary and b) real part of  $\sigma(\omega)$  of 15 nm NbN film on MgO substrate ( $T_c = 15.4$  K). Solid lines are fits with the BCS equations [29]. Inset to a) shows the transmitted THz transients through the NbN film below and above  $T_c$ ; the arrow denotes the time  $t' = t_0$  with maximum change in the transmitted electric field. Inset to b): the T-dependence of  $\Delta$ , extracted from fits to  $\sigma(\omega)$  (symbols) overlaying the normalized transmissivity ratio, TR. The BCS T-dependence of  $\Delta$  is shown by the dashed line.

Fig. 1 presents the T-dependence of  $\sigma(\omega)$  of a 15 nm NbN film with  $T_c = 15.4$  K. In the normal state  $\sigma(\omega)$  is fit with the Drude model with the plasma frequency  $\nu_p = 460$  THz ( $15300 \text{ cm}^{-1}$ ) and the scattering rate  $\hbar/\tau = 264 \text{ cm}^{-1}$ , in good agreement with studies on thick films [33]. In the SC state an excellent agreement between the data and  $\sigma(\omega)$  using the BCS model with a finite normal state scattering rate [29] (solid lines) is obtained. The extracted T-dependence of  $\Delta$ , with  $\Delta(0) \approx 0.75$  THz ( $3.07 \text{ meV}$ ) and  $2\Delta/k_B T_c \approx 4.6$ , is shown in inset to panel b).  $\Delta(T)$  is plotted on top of TR, the transmissivity ratio  $\mathcal{T}(\omega, T)/\mathcal{T}(\omega, 16\text{K})$ , which

is at each T normalized to its peak value (in a BCS SC, the transmissivity ratio peaks just above  $2\Delta$  [33]).

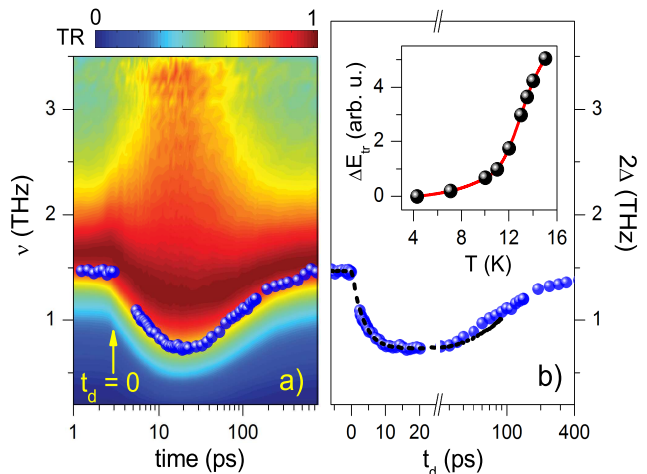


FIG. 2: (color online) a) The time evolution of normalized transmissivity ratio (TR), recorded at  $A = 22 \text{ mJ}/\text{cm}^3$ , together with  $\Delta(t)$  extracted from  $\sigma_1(\omega, t_d)$  fit with the BCS formula [29]. b) Comparison of  $\Delta(t_d)$  extracted from  $\sigma_1(\omega, t_d)$  (symbols) and from the spectrally integrated response  $\Delta E_{tr}(t_0, t_d)$  (dashed line). Inset: the measured T-dependence of  $\Delta E_{tr}(t_0)$  used to relate  $\Delta E_{tr}(t_0, t_d)$  to the change in  $\Delta$ .

Fig. 2a) presents the temporal evolution of TR following photoexcitation with a 50 fs optical pulse with  $A = 22 \text{ mJ}/\text{cm}^3$ . The data reveal a strong suppression of SC on the 10 ps time scale followed by the recovery on the 100 ps timescale. On the same plot  $\Delta(t_d)$ , obtained by best fit to  $\sigma_1(\omega, t_d)$  using the BCS model [29] is plotted by solid symbols.

To perform systematic studies of the time evolution of  $\Delta$  as a function of  $A$  and T, avoiding the signal drifts associated with the long term laser stability, we studied the dynamics of the induced changes in the transmitted electric field,  $\Delta E_{tr}(t')$ , at a fixed point of  $E_{tr}(t' = t_0)$ . The fixed point of  $E_{tr}(t_0)$  in these experiments was at the point of maximum time derivative of the electric field,  $t_0 = 0$  ps, where the changes in  $E_{tr}(t_0)$  upon entering the SC state are the largest – see inset to Fig. 1a). In order to obtain a direct link between  $\Delta E_{tr}(t_0)$  and the photoinduced change of the gap,  $\delta\Delta$ , we first measured  $\Delta E_{tr}(t_0, T, T_0) = E_{tr}(t_0, T) - E_{tr}(t_0, T_0)$ , where  $T_0$  is the T of the sample at which photoinduced studies are performed. Combining  $\Delta E_{tr}(t_0, T, 4.3\text{K})$ , shown in inset to Fig. 2b), with the T-dependence of the gap (inset to Fig. 1b)) enabled us to extract the temporal evolution of the gap from  $\Delta E_{tr}(t_0, t_d)$  traces. The trace obtained this way at  $A = 22 \text{ mJ}/\text{cm}^3$ , shown by the dashed curve in Fig. 2b), matches well the time evolution of the gap extracted from the  $\sigma_1(\omega, t_d)$  data. Therefore, by measuring the spectrally integrated response, the T- and A-

dependence of the photoinduced gap change,  $\delta\Delta$ , can be extracted quickly, avoiding system drifts.

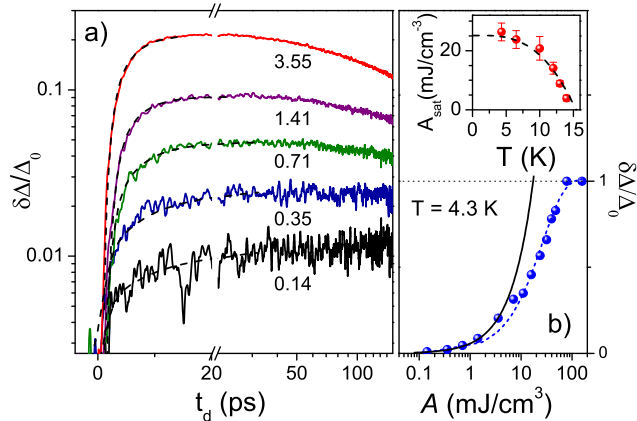


FIG. 3: (color online) a) The relative change in gap,  $\delta\Delta/\Delta_0$  recorded at 4.3 K for various  $A$  in  $\text{mJ}/\text{cm}^3$ . The dashed lines are fits to the data with Eq.(1). b) The dependence of  $\delta\Delta/\Delta_0$  on  $A$  at 4.3 K. The dashed line is a fit to the simple saturation model, the solid line is the linear fit. Inset: The T-dependence of the saturation energy density,  $A_{sat}$ , compared to the T-dependence of  $\Delta^2$  (dashed line).

Fig. 3a) presents the  $\delta\Delta(t_d)$  traces for various  $A$  recorded at 4.3 K. As shown in Fig. 3b) the maximum induced change initially increases linearly with excitation density, followed by a saturation resulting from suppression of SC. To estimate the characteristic  $A$  required to suppress SC, we use a simple saturation model,  $\delta\Delta/\Delta_0 = (1 - \exp(-A/A_{sat}))$ . Here  $A_{sat}$  is the characteristic absorbed energy density required to suppress SC and is  $A_{sat}(4.3 \text{ K}) \approx 25 \text{ mJ}/\text{cm}^3$ . We find that in NbN  $A_{sat}$  is, within the experimental accuracy, comparable to the thermodynamic SC condensation energy,  $E_c = 22 \text{ mJ}/\text{cm}^3$ . Here  $E_c = B_c^2/2\mu_0 = N(0)\Delta^2/2$ , with  $B_c = 0.234 \text{ T}$  [28] being the thermodynamic critical field and  $N(0)$  the single spin density of states at the Fermi level. As shown in inset to Fig. 3b), the T-dependence of  $A_{sat}$  is found to follow the T-dependence of  $\Delta^2$  (dashed line). These observations are in strong contrast to similar studies in cuprates [11, 13, 14], where  $A_{sat}$  is found to be about one order of magnitude higher than  $E_c$  and nearly T-independent [14].

As demonstrated in Fig. 3a), both the CPB and the SC recovery show pronounced dependence on  $A$ . The CPB rate is found to increase with increasing  $A$ , similarly to the case of  $\text{MgB}_2$  [26]. This behavior can be attributed to the intrinsic non-linearity of the SC state relaxation process, where the populations of the photoexcited QP and the high frequency ( $\hbar\omega > 2\Delta$ ) phonon (HFP) densities are described by the coupled RT rate equations [3, 20, 26]. Here the long timescale of the CPB implies that photoexcited hot electrons (holes) initially generate a high density of HFP, which subsequently break Cooper

pairs until the quasi-equilibrium between QP and HFP populations is reached [20, 26].

The CPB can be quantitatively analyzed using the RT model. In the low photoexcitation limit ( $\delta\Delta \ll \Delta$ ), where the RT analysis is applicable,  $\delta\Delta$  is proportional to the photoexcited QP density,  $n_{PI}$ . It is easy to show that at 4K  $n_{PI}$  is for the entire range of  $A$  substantially higher than the density of thermally excited QP,  $n_T$ . From  $n_T \approx N(0)\sqrt{2\pi\Delta k_B T} \exp(-\Delta/T)$ , where  $N(0) = 0.44 \text{ spin}^{-1}\text{unit cell}^{-1} \text{ eV}^{-1}$ , [36] it follows that  $n_T(4 \text{ K}) \approx 1 \cdot 10^{-6} \text{ unit cell}^{-1}$  while  $A = 0.14 \text{ mJ}/\text{cm}^3$  corresponds to  $n_{PI} \approx 3 \cdot 10^{-5} \text{ unit cell}^{-1}$ . Therefore, the CPB ( $t_d \lesssim 20 \text{ ps}$ ), which is well separated from the SC state recovery dynamics ( $\gtrsim 100 \text{ ps}$ ), can be fit (dashed lines in Fig. 3a)) with [20, 26]

$$n_{PI}(t_d) = \frac{\beta}{R} \left[ -\frac{1}{4} - \frac{1}{2\tau} + \frac{1}{\tau} \frac{1}{1 - K \exp(-t_d\beta/\tau)} \right]. \quad (1)$$

Here  $\beta$  is the CPB probability by absorption of HFP,  $R$  is the bare QP recombination rate, while  $K$  and  $\tau$  are dimensionless parameters (Eq.(3) of Ref.[26]) determined by  $\beta$ ,  $R$  and the initial conditions (the ratio of the absorbed energy in the HFP and QP subsystems following the initial e-e and e-ph scattering of hot electrons (holes)), which should be independent on  $A$  for these low excitation densities [20, 26]. The extracted dependences of  $\tau/\beta$  and  $K$  on  $A$  are shown in Figs. 4a) and 4b), together with the fit with Eqs.(3) of Ref.[26] (dashed lines). The best fit is obtained when 91 % of  $A$  is initially transferred to the HFP subsystem, giving the values of the microscopic constants  $\beta^{-1} = 6 \pm 1 \text{ ps}$ ,  $R = 160 \pm 20 \text{ ps}^{-1}\text{unit cell}$ .

Fig. 4c) presents the dependence of the SC recovery time,  $\tau_{rec}$ , on  $T$  and  $A$ . Here  $\tau_{rec}$  is obtained by fitting the recovery dynamics with a single exponential decay. As shown in inset to Fig. 4c), at 4 K  $\tau_{rec}^{-1}$  first increases linearly with  $A$ , mimicking the intrinsic bimolecular kinetics of the QP recombination [20]. For  $A \gtrsim 5 \text{ mJ}/\text{cm}^3$  and for  $T > 10 \text{ K}$   $\tau_{rec}^{-1}$  is constant at  $\tau_{rec}^{-1}(0) \approx 0.01 \text{ ps}^{-1}$ . In NbN  $\tau_{rec}^{-1}(0)$  is governed by the escape of the HFP into the substrate and is inversely proportional to the film thickness [34]. It was argued that the dependence of  $\tau_{rec}$  on  $A$ , observed in cuprates, implies the absence of the phonon bottleneck in cuprates [8, 9]. The subsequent analysis of the RT model [20], however, suggested a (perhaps counterintuitive) result, that also in a phonon bottleneck case  $\tau_{rec}^{-1} \propto n_{PI}$  for  $n_T < n_{PI} \leq \beta/R$ . Here  $\beta/R$  is the material dependent characteristic QP density, below which the RT perturbative description is applicable [20]. Indeed,  $A = 5 \text{ mJ}/\text{cm}^3$  corresponds to  $n_{PI} \approx 0.001 \text{ unit cell}^{-1}$ , identical to  $\beta/R \approx 0.001 \text{ unit cell}^{-1}$  determined from the analysis of the CPB. Similarly, the fact that  $\tau_{rec}^{-1}$  is above  $\approx 10 \text{ K}$  A- and T-independent follows from the fact that  $n_T(10\text{K}) \approx 0.0003 \text{ unit cell}^{-1}$  is comparable to  $\beta/R$ . Therefore, as experimentally demonstrated here for a standard BCS SC, the A-dependent

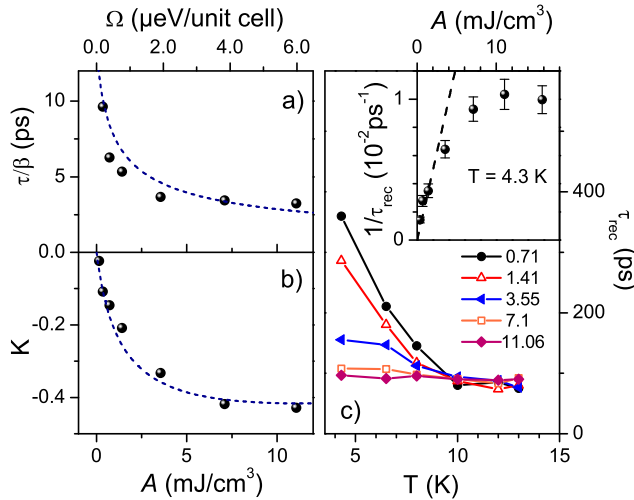


FIG. 4: (color online) Panels a) and b) show the dependence of  $\tau/\beta$  and  $K$  on  $A$ ; the values are extracted from fits to the Cooper pair breaking dynamics (Fig. 3a). Panel c) shows the T-dependence of the SC recovery time,  $\tau_{rec}$ , for several  $A$  (in mJ/cm<sup>3</sup>). Inset:  $\tau_{rec}^{-1}(A)$  recorded at 4.3 K. For low  $A$  the relaxation rate increases linear with  $A$  (dashed line).

SC state recovery at low Ts seems to be an intrinsic feature of a SC driven out of equilibrium, and should be observed in the phonon bottleneck case, providing that  $n_T < n_{PI} \leq \beta/R$ . Based on this study, we argue that it is the absence of  $A$ -dependence of the SC state recovery, observed e.g. in optimally doped YBCO [5] and in an overdoped BSCCO [8], that presents an anomalous behavior and not vice versa as argued [8, 9].

As demonstrated, the dynamics of photoexcited NbN can be over large range of T and  $A$  well described by the phenomenological RT model, enabling us to determine the values of microscopic parameters  $R$  and  $\beta$ . Since  $R = \frac{8\pi\lambda\Delta^2}{\hbar N(0)\Omega_c^2}$  [6, 35], where  $\Omega_c$  is the phonon cut-off frequency, the value of  $\lambda$  can be determined. Taking the known values for  $\Delta$ ,  $N(0)$  and  $\Omega_c = 16$  THz [28], we obtain  $\lambda = 1.1 \pm 0.12$ , which is in a very good agreement with the theoretical estimates,  $\lambda = 1 - 1.12$  [36, 37]. Importantly, such an approach does not suffer from the (ambiguous) underlying assumptions of the two-temperature model, the model commonly [10, 18] used to determine  $\lambda$ .

In summary, we presented the first systematic studies of the SC state relaxation phenomena in a conventional BCS superconductor NbN with ps time-resolution. Utilizing the TDTS, we were able to study the time evolution of  $\Delta$  over large range of temperatures and excitation densities. We demonstrated, that both the CPB and SC state recovery dynamics depend strongly on the excitation density in agreement with the predictions of the phenomenological RT model [20, 26]. Studying the CPB enabled us to determine the values of the microscopic parameters  $R$ ,  $\beta$ , as well as the dimensionless e-ph coupling

constant  $\lambda$  in NbN. This approach could be used to determine the electron-boson coupling strengths in high- $T_c$  SCs, providing the CPB dynamics as a function of excitation density can be experimentally resolved. Last but not least, our results on NbN emphasize the unusual nature of the  $A$ -independent relaxation observed in some cuprates [5, 8].

This work was supported by the German Israeli DIP project No. 563363, Alexander von Humboldt Foundation, Zukunftskolleg and Center for Applied Photonics at the University of Konstanz.

- [1] E. Burstein, D. N. Langenberg, and B. N. Taylor, *Phys. Rev. Lett.* **6**, 92 (1961).
- [2] D. M. Ginsberg, *Phys. Rev. Lett.* **8**, 204 (1962).
- [3] A. Rothwarf, B.N. Taylor, *Phys. Rev. Lett.* **19**, 27 (1967).
- [4] S.G. Han, *et al.*, *Phys. Rev. Lett.* **65**, 2708 (1990).
- [5] V.V. Kabanov, *et al.*, *Phys. Rev.* **B 59**, 1497 (1999).
- [6] J. Demsar, *et al.*, *Phys. Rev.* **B 63**, 054519 (2001).
- [7] R.D. Averitt, *et al.*, *Phys. Rev.* **B 63**, 140502(R) (2001).
- [8] N. Gedik, *et al.*, *Phys. Rev. Lett.* **95**, 117005 (2005).
- [9] R.A. Kaindl, *et al.*, *Phys. Rev.* **B 72**, 060510 (2005).
- [10] L. Perfetti, *et al.*, *Phys. Rev. Lett.* **99**, 197001 (2007).
- [11] P. Kusar, *et al.*, *Phys. Rev. Lett.* **101**, 227001 (2008).
- [12] C. Giannetti, *et al.*, *Phys. Rev.* **B 80**, 235129 (2009).
- [13] A. Pashkin, *et al.*, *Phys. Rev. Lett.* **105**, 067001 (2010).
- [14] M. Beyer, *et al.*, *Phys. Rev.* **B 83**, 214515 (2011).
- [15] R. Cortés, *et al.*, *Phys. Rev. Lett.* **107**, 097002 (2011).
- [16] T. Mertelj, *et al.*, *Phys. Rev. Lett.* **102**, 117002 (2009).
- [17] E.E.M. Chia, *et al.*, *Phys. Rev. Lett.* **104**, 027003 (2010).
- [18] B. Mansart, *et al.*, *Phys. Rev.* **B 82**, 024513 (2010).
- [19] D.H. Torchinsky, *et al.*, *Phys. Rev. Lett.* **105**, 027005 (2010).
- [20] V.V. Kabanov, J. Demsar, D. Mihailovic, *Phys. Rev. Lett.* **95**, 147002 (2005).
- [21] E. J. Nicol and J. P. Carbotte, *Phys. Rev.* **B 67**, 214506 (2003).
- [22] P. C. Howell, A. Rosch, P. J. Hirschfeld, *Phys. Rev. Lett.* **92**, 037003 (2004).
- [23] A. Dienst, *et al.*, *Nature Photon.* **5**, 485 (2011).
- [24] J.F. Federici, *et al.*, *Phys. Rev.* **B 46**, 11153 (1992).
- [25] G.L. Carr, *et al.*, *Phys. Rev. Lett.* **85**, 3001 (2000).
- [26] J. Demsar, *et al.*, *Phys. Rev. Lett.* **91**, 267002 (2003).
- [27] R.P.S.M. Lobo, *et al.*, *Phys. Rev.* **B 72**, 024510 (2005).
- [28] C. Geibel, *et al.*, *J. Phys. F: Met. Phys.* **15**, 405 (1985).
- [29] W. Zimmermann, *et al.*, *Physica C* **183**, 99 (1991).
- [30] The diameter depends on frequency, ranging from 0.22 mm (3 THz) to 1.3 mm (0.3 THz).
- [31] G. Gol'tsman, *et al.*, *Appl. Phys. Lett.* **79**, 705 (2001).
- [32] M. Beck, *et al.*, *Opt. Express* **18**, 9251 (2010).
- [33] H. S. Somal, *et al.*, *Phys. Rev. Lett.* **76**, 1525 (1996).
- [34] K.S. Il'in, *et al.*, *Appl. Phys. Lett.* **76**, 2752 (2000).
- [35] Yu. N. Ovchinnikov and V.Z. Kresin, *Phys. Rev.* **B 58**, 12416 (1998).
- [36] W. Weber, *Phys. Rev.* **B 8**, 5082 (1973).
- [37] U. Haufe, G. Kerker and K.H. Bennemann, *Sol. Stat. Comm.* **17**, 321 (1975).